Abundant Taxa and Favorable Pathways in the Microbiome of Soda-Saline Lakes in Inner Mongolia

Dahe Zhao
Institute of Microbiology Chinese Academy of Sciences
Shengjie Zhang
Institute of Microbiology Chinese Academy of Sciences
Qiong Xue
Institute of Microbiology Chinese Academy of Sciences
Junyu Chen
Institute of Microbiology Chinese Academy of Sciences
Jian Zhou
Institute of Microbiology Chinese Academy of Sciences
Feiyue Cheng
Institute of Microbiology Chinese Academy of Sciences
Ming Li
Institute of Microbiology Chinese Academy of Sciences
Yaxin Zhu
Institute of Microbiology Chinese Academy of Sciences
Haiying Yu
Beijing Institute of Genomics Chinese Academy of Sciences
Songnian Hu
Institute of Microbiology Chinese Academy of Sciences
Yanning Zheng
Institute of Microbiology Chinese Academy of Sciences
Shuangjiang Liu
Institute of Microbiology Chinese Academy of Sciences
Hua Xiang (xiangh@im.ac.cn)
Institute of Microbiology Chinese Academy of Sciences https://orcid.org/0000-0003-0369-1225

Research

Keywords: Soda-Saline lakes, Deep metagenomic sequencing, Microbiome, Abundant taxa, Sulfur cycling, Glucan metabolism

Posted Date: December 18th, 2019

DOI: https://doi.org/10.21203/rs.2.19124/v1

Abstract

Background: The chloride-carbonate-sulfate lakes (also called Soda-Saline lakes) are double-extreme ecological environments with high pH and high salinity values but can also exhibit high biodiversity and high productivity. The diversity of metabolic process that functioned well in such environments remains to be systematically investigated. Deep sequencing and species-level characterization of the microbiome in elemental cycling of carbon and sulfur will provide novel insights into the microbial adaptation in such saline-alkaline lakes.

Results: In this study, we characterized environmental factors and performed deep metagenomic sequencing of the brine and sediment samples from nine ponds with different salinities of two chloride-carbonate-sulfate lakes in Inner Mongolia of China. The results showed that the concentration of chloride most significantly influenced the microbial community in both of the brine and sediment environments. Of 385 high-quality metagenome-assembled genomes (MAGs) belonging to archaea (56 Euryarchaeota, 12 Candidatus Nanohaloarchaeota, and 12 Candidatus Woesearchaeota) and bacteria (119 Proteobacteria and 186 other diverse bacterial phyla, including 18 from Candidate Phyla Radiation, CPR), 38 MAGs were observed to be abundant species at least in one of the eighteen niches. These abundant taxa represented most branches of a phylogenomic tree at phylum level. Interestingly, almost half of the abundant MAGs had the potential to drive dissimilatory sulfur cycling, including four autotrophic Ectothiorhodospiraceae MAGs, one Cyanobacteria MAG and nine heterotrophic MAGs with potential to oxidize sulfur, as well as four abundant MAGs containing genes for elemental sulfur respiration, which may increase the ability of environmental adaptation in such saline-alkaline environments. In addition, some subgroups in Ca. Nanohaloarchaeota and Ca. Woesearchaeota of the DPANN superphylum were also observed abundant. We found 1,4-alpha-glucans phosphorylation and complete glycolysis pathway in the abundant Nanohaloarchaeota MAG NHA-1, and this efficient energy regeneration pathway (compared with hydrolysis) may be a key factor for Ca. Nanohaloarchaeota in adaptation to hypersaline environments.

Conclusions: The abundant taxa including carbon fixing microbes, versatile heterotrophs and the nanosized DPANN superphyla, and the superiority of energy production and thermodynamics of these abundant species were systematically investigated. This has provided novel insights into the microbial process in chloride-carbonate-sulfate lakes, and further understanding of the metabolic mechanism of adaptation to such extremely alkaline and saline conditions.

Background

Soda lakes are a type of saline lake with extremely high pH and salinity due to high concentrations of carbonate/bicarbonate and many other inorganic salts (1). Under alkaline and saline conditions, microbial activities are rather high, including surprisingly high biodiversity (2–5), relatively high primary productivity rates (6–10), vigorous oxidation and reduction reactions of sulfur (11–15), and elevated biochemical cycling of various compounds and elements (16–19). High concentrations of inorganic ions

such as (bi)carbonate and phosphate provide adequate essential elements, while some intermediate metabolites (e.g., hydrogen sulfide) exhibit low toxicity under alkaline conditions (20). Regardless, microbes inhabiting extreme environments, especially abundant ones, function in the elemental cycling of carbon, sulfur and nitrogen (21).

In the brines of alkaline soda lakes, Bacteroidetes, Alphaproteobacteria, Gammaproteobacteria, and Euryarchaeota were identified as taxa with the highest levels of abundance at different salinities (from 170 to 400 g/L) by both amplicon sequencing of 16S rRNA gene and direct metagenomic sequencing (22). The genomes of haloalkaliphilic members of the Candidate Phyla Radiation (CPR) and several hundred other novel prokaryote lineages were obtained from the metagenomic assembly of sequences from the sediment of soda lakes, while the Wood-Ljungdahl pathway for carbon fixation was detected in more taxonomic groups from the same samples (23). The autotrophic microbial community based on the detection of molecular markers (ribulose-1,5-bisphosphate carboxylase (RuBisCO) and ATP citrate lyase (Acl) in the CBB and rTCA cycles, respectively) indicated that haloalkaliphilic cyanobacteria and sulfur oxidizing bacteria of the genus Halorhodospira were predominant in soda lakes (24, 25). Interestingly, even alkaline soda lakes separated by a large distance between Asia and North America were shown to share a similar core microbiome (8).

Although a multilevel strategy has been proposed, cytoplasmic neutral pH homeostasis and osmotic regulation have been shown to be significant factors in the adaptation of microbes to alkaline and saline environments, respectively (26). The biosynthesis or uptake of compatible solutes (such as glycine betaine and ectoine) by halophilic and haloalkaliphilic bacteria are commonly used as the primary mechanism to resist the extracellular osmotic pressure (27). Haloarchaea and anaerobic Natranaerobiaceae have been reported to primarily maintain osmotic balance using K^+ and Cl^- import systems (28). The monovalent cation/proton antiporters, widely present in archaea and bacteria, function in intracellular pH homeostasis (29). Importantly, microbes must consume a great deal of energy to respond to extreme conditions.

There are hundreds of small soda lakes and pans in the Inner Mongolia Autonomous Region, China (30). Analysis of the physicochemical factors in these lakes indicated that many of them are soda-saline lakes of chloride-carbonate-sulfate type, which providing an excellent system for studying the coupling of carbon-sulfur cycling and the microbial environmental adaptation. In this study, we collected brine and sediment samples from nine ponds associated with two lakes and performed deep metagenomic sequencing. Combined with environmental characterizations, we dissected the microbial community structures and relationships based on metagenomic reads and assembled genomes, subsequently focusing on the abundant species representing most branches of a phylogenomic tree. The putative physiochemical characteristics and ecological functions of MAGs with high coverage, including carbon fixing microbes, versatile heterotrophs and the nanosized DPANN superphyla were analyzed. The superiority of energy production and thermodynamics in the abundant species was assessed to further understand the metabolic mechanism of adaptation to such extremely alkaline and saline conditions.

Results

Multiple environmental factors shape microbial community composition

Habor Lake (DK) and Hutong Qagan Lake (HC) are located in the southwest of Inner Mongolia Autonomous Region of China (Fig. S1a) and comprise numerous ponds with various salinities and a typical depth of 1-5 meters. Brine and sediment samples of four DK ponds (DK15, DK20, DK27, and DK32) and five HC ponds (HC5, HC27, HC17, HC22, and HC26) were collected (Fig. S1b and c). The salinities of these ponds ranged from 5.5% to saturation, with pH values that were generally higher than 9.8. The concentrations of CO_3^{2-} and HCO_3^- ranged from 78.33 to 820 mM and from 80.33 to 385.25 mM, respectively, while the concentrations of chloride were much higher than (bi)carbonate. Therefore, both DK and HC were classified as Soda-Saline lakes of the chloride-carbonate-sulfate type (31), and will simply called Soda-Saline lakes in the following statement . The values obtained for additional physicochemical parameters (magnesium ion, calcium ion, chloride, sulfate, phosphate, ammonia and total organic nitrogen concentrations) are shown in Table S1.

Brine and sediment samples from the nine ponds were used to perform deep metagenomic sequencing (Table S2). The average number of raw bases for the 18 samples was 15.98 Gb, with 281.05 Gb of clean data obtained after quality filtering. The bioinformatics analyses described below were performed using these metagenomes.

The microbial community composition was determined based on the taxonomy assignment of total non-redundant gene catalog acquired from metagenomics assembly, open reading frame (ORF) prediction and redundancy remove, and the influences of environmental factors were analyzed by redundancy analysis (RDA) based on the microbial composition of 18 samples in the genus level. The brine and sediment samples separated in the RDA (Fig. 1a), suggesting that the microbial community structures in the two sample types were significantly different. This conclusion was also supported by the principal component analysis (PCA) results (Fig. S3a), whereas the microbial community structures in the DK and HC samples (different lakes) were generally similar (Fig. S3b). For species diversity, the Shannon-Weaver index value obtained for the sediment was much higher than that observed for the brine (Fig. S4a). Again, the overall biodiversity in the DK and HC was similar (Fig. S4b). For physicochemical factors, the Cl^- concentration was the most influential environmental factor determining microbial composition (Fig. 1a), to which pH, salinity, CO_3^{2-}, HCO_3^-, SO_4^{2-} and conductivity were positively correlated (Fig. 1a and Fig. S2).

We further assessed the microbial taxonomic profiles at the phylum level and their relative abundances in each of the samples based on the classification of nonredundant genes by alignment against the NCBI nr database (Fig. 1b). Sixteen phyla were observed in abundance (>0.1%) (Table S3). *Proteobacteria* (bacteria) and/or *Euryarchaeota* (archaea) constituted the majority of phyla across the 18 samples. In brine samples, the abundance of *Proteobacteria* ranged from 13.6 to 31.5% in samples HC5W, DK15W, HC17W, HC27W, DK20W and HC22W with relatively low Cl^-, whereas this abundance reached no more than 5.5% in water samples containing extremely high Cl^- levels (HC26W, DK27W, and DK32W). In

contrast, the abundance of *Euryachaeota* increased from 0.1 to 41.7% along with the increase in the Cl^- concentration. *Proteobacteria* and *Euryarchaeota* were also the most abundant phyla in sediment samples. In addition, *Firmicutes*, *Actinobacteria*, *Bacteriodetes*, *Cyanobacteria* and Ca. *Nanohaloarchaeota* were all detected in abundance in Soda-Saline lakes (Fig. 1b).

Metagenome-assembled genomes revealed abundant species

To determine the microbial composition and putative ecological function, the metagenome-assembled genomes (MAGs) were binned. We obtained 385 high-quality MAGs (completeness>90% and contamination<10%, completeness>80% and contamination<5, or completeness>50% and contamination <2%) from 27 archaeal and bacterial phyla (Fig. 2, Table S4). The naming convention of MAGs was the abbreviation of class (in *Proteobacteria*), phylum (most phyla), or superphylum (CPR) with serial number (Table S4). Of the 79 archaeal MAGs, 55 belonged to *Euryarchaeota*, while the remaining belonged to Ca. *Nanohaloarchaeota* (12 MAGs) and Ca. *Woesearchaeota* (12 MAGs). Of the 55 *Euryarchaeota* MAGs, 48 MAGs were from the class *Halobacteria* and 7 were from the classes *Methanomicrobia*, *Methanonatronarchaeia*, *Thermoplasmata* and unclassified *Euryarchaeota* (Table S4). In bacteria, most MAGs belonged to the phyla *Proteobacteria* (119 MAGs), *Firmicutes* (33 MAGs), *Bacteroidetes* (29 MAGs) and *Actinobacteria* (20 MAGs). Additionally, many other diverse MAGs were obtained, including *Balneolaeota*, *Tenericutes*, *Verrucomicrobia*, *Cyanobacteria*, *Spirochaetes*, and CPR (Fig. 2, Table S4).

The relative abundances of the 385 MAGs in the 18 samples are shown in Fig. 3. The microbiomes of the 18 brine and sediment samples comprised a small number of abundant species (relative abundance >50% of MAGs with the highest coverage in the same niche) and a large number of rare MAGs (Fig. 3). We observed more abundant bacterial MAGs in brine and sediment samples with relatively low chloride and salinity, especially *Gammaproteobacteria*, *Deltaproteobacteria*, *Alphaproteobacteria*, *Actinobacteria*, and *Tenericutes*. Cyanobacteria MAG CB-1 was found to be abundant in the brine with the lowest concentration of chloride (Fig. 4). Two CPR MAGs were found in abundance, including CPR-1 in DK15W and CPR-2 in HC27S (Fig. 4). Some bacterial MAGs were abundant in relatively high chloride samples, such as *Deltaproteobacteria* MAG DPB-4 and *Gammaproteobacteria* MAG GPB-6 in HC26W, BB-1 in HC26S (Fig. 4). Interestingly, GPB-6 (*Spiribacter* sp.) was shown to be an abundant microbe in brine and/or sediment samples from five ponds with different salinities (Fig. 4), suggesting that GPB-6 exhibited excellent adaptation to alkaline and saline environments. In agreement with this observation, previous study has showed that *Spiribacter salinus* M19-40 is one of the most predominant bacteria in neutral saline lakes (32), and the streamlined genome of this bacterium is considered to provide significant advantage in environemtal adaptation (33). We also observed archaeal MAGs were abundant in samples with relatively highest salinities, including *Euryarchaeota*, Ca. *Nanohaloarchaeota* and Ca. *Woesearchaeota* (Fig. 4).

The total of 38 abundant MAGs were marked (with five-pointed star) in the phylogenomic tree based on the alignment of universal proteins across *Bacteria* and *Archaea* (Fig. 2). Although these abundant MAGs accounted only about 10% of the total MAGs, they were from 13 phyla representing half of biodiversity at phylum level (Table S7), and accounting 24.81-69.23% of total coverages of 385 MAGs in 18 samples (Table S5). Therefore, they were ideal taxa to understand the microbial functions and adaptation mechanisms in these specific alkaline chloride-carbonate-sulfate niches. To achieve this, we have summarized the metabolic potential of these abundant MAGs in Table S6.

Widely spreading of sulfur oxidation in autotrophic and heterotrophic bacteria

A total of 18 abundant MAGs have the potential to drive the dissimilatory cycling of elements sulfur, and sulfide oxidation was present in 14 MAGs. In the autotrophic *Ectothiorhodospiraceae* family, two MAGs (GPB-4 and GPB-5) encoded bacterial photosynthetic reaction center and marker genes (*prk* encoding phosphoribulokinase, *rbcLS* encoding ribulose-bisphosphate carboxylase large and small chain) of the CBB cycle, and were both abundant in the sediment of HC27 (Fig. 4). Considering the potential for light energy utilization and anoxygenic photosynthetic lifestyle in these species, they may be dominant carbon fixing microbes at the surfaces of sediment. GPB-5 was observed to encode sulfide:quinone oxidoreductase (Sqr), flavocytochrome c sulfide dehydrogenase (FccB), reversed dissimilatory sulfite reductase (rDsrAB), and sulfite dehydrogenase (SoeABC) (Table S6), exhibiting the metabolic potential to oxidize multiple sulfur compounds (Fig. 4). GPB-5 was predicted to belong to the genus *Halorhodospira* and may be an anoxygenic purple sulfur bacterium. GPB-4 was identified as an unclassified member of the family *Ectothiorhodospiraceae* and did not show the capability of oxidizing sulfur compounds or hydrogen (Table S6). However, considering that the completeness of the MAG GPB-4 was relatively low (67.44%), partial genes encoding sulfur-oxidizing proteins (SoxBYZ), SoeC, coenzyme F420 hydrogenase subunit beta and hydrogenase expression/formation proteins in GPB-4 may indicate a putative ability of this organism to oxidize sulfur compound or hydrogen (Table S6). Notably, both GPB-4 and GPB-5 had the nitrogenase genes *nifHDK* (Table S6), indicating that they may be involved in nitrogen fixation in pond HC27. Two *Thioalkalivibrio* MAGs (GPB-7 and GPB-8) and one *Thiohalomonas* MAG (GPB-10) were abundant in sediment samples from ponds HC17, DK15 and HC5, respectively (Fig. 4). These three MAGs had marker genes for the CBB cycle and the oxidization or disproportionation of multiple sulfur compounds (Table S6), consistent with the metabolic characteristics of *Thioalkalivibrio* and *Thiohalomonas*. Apart from carbon fixation and sulfur cycling, GPB-7 and GPB-8 contained hydrogenase genes and may utilize hydrogen as energy source and reducing power, while GPB-10 harbored *nifHDK* genes (Table S6) and exhibited the potential to fix nitrogen (Fig. 4). In short, our results support that carbon fixing and sulfur oxidation were coupled in these anoxygenic photosynthetic and chemolithotrophic *Ectothiorhodospiraceae* species.

Besides, eight cyanobacterial MAGs were obtained, while only one MAG (CB-1) belonging to the Cyanobacterial genus *Arthrospira* was detected as an abundant species in the brine of HC5 (Table S4),

which had the lowest salinity and chloride concentrations (Fig. 4). Cyanobacteria are typically the primary contributors to carbon fixation. CB-1 encoded Prk and RbcLS, and the complete photosystems II and I (Table S6), indicating that it has the potential to photosynthetically fix carbon via the CBB cycle (Fig. 4). This MAG also encoded hydrogenase, nitrate reductase, and Sqr, exhibiting versatile metabolic capabilities. Four other cyanobacterial MAGs had the potential to perform photosynthesis, of which three encoded Sqr and two encoded nitrogenase (Table S6). It was interesting to note that under alkaline conditions, most photosynthetic *Cyanobacteria* MAGs had the potential to oxidize sulfide (Table S6), that may regulate the photosynthesis and carbon fixing (34).

Interestingly, we observed that many abundant bacteria from heterotrophic taxa also harbored Sqr, including AB-1 and AB-3 from *Actinobacteria*, CF-1 from *Chloroflexi*, APB-1 and APB-2 from *Alphaproteobacteria*, DPB-4 from *Deltaproteobacteria*, and GPB-1, GPB-2 and GPB-9 from *Gammaproteobacteria* (Figs. 2 and 4), indicating their potential in oxidation-mediated detoxification of sulfide with various salinities in the saline-alkaline environments. In addition, four *Halobacteria* MAGs EA-2, EA-4, EA-5 and EA-6 harboring thiosulfate dehydrogenase [quinone] large subunit (*doxD*) allowing for potential thiosulfate oxidation (Table S6). Sulfide and thiosulfate could provide accessory energy under nutrient limited conditions to heterotrophs, and increase the growth rate and flux of assimilatory carbon via anaplerotic reaction of oxaloacetate (discuss below). This lifestyle is considered as facultative lithoheterotrophy (35).

Reduction of sulfur compounds makes sulfur cycling complete

As so many autotrophic and heterotrophic abundant MAGs exhibited the potential to oxidize reductive sulfur compounds (RSCs), it would be interesting to investigate whether there were considerable sulfur reducing microbes to complete the sulfur cycling in the chloride-carbonate-sulfate lakes. Notably, we found the presence of anaerobic respiration processes in abundant MAGs, including sulfur respiration (Fig. 4). *Halorubrum* spp. EA-4, EA-5, *Halarsenatibacter* sp. FB-1, *Desulfonatronospira* sp. DPB-1 had the *psrA/phsA* gene (Table S6), allowing for potential polysulfide reduction/thiosulfate disproportionation. The *Desulfonatronospira* MAG DPB-1 was an abundant species in the sediment of HC17 (Fig. 4) and encoded thiosulfate reductase/polysulfide reductase chain A (*psrA/phsA*) and F420-non-reducing hydrogenase subunits (*mvhADG*) (Table S6), indicating the lifestyle of chemolithotrophic sulfate-reducing bacterium. It is noteworthy that DPB-1 also had the marker genes of anaerobic carbon-monoxide dehydrogenase catalytic subunit (*cooS*), acetyl-CoA synthase (*acsB*), and acetyl-CoA decarbonylase/synthase subunits (*cdhDE*) in the WL pathway (Table S6), indicating that it may fix inorganic carbon via the WL pathway.

Not only elemental sulfur reduction, we also observed the potential of sulfate/sulfite and tetrathionate reduction in many MAGs. Seven MAGs from *Desulfobacterales* and *Desulfovibrionales* harbored dsrAB gene for sulfate/sulfite respiration, and some of them had the potential of carbon fixing (Table S6). The type strains from same taxonomies were reported facultative autotrophs with hydrogen and/or formate

as substrates (36-40). *Halomonas* sp. GPB-59, *Marinobacter* sp. GPB-11, and *Aquisalimonas* sp. GPB-38 harbored *ttrABC* genes for tetrathionate reductase, while other five MAGs from *Actinobacter* and one *Desulfuromusa* MAG had *ttrAB* (Table S6), with potential of tetrathionate respiration. Although the abundance was not high, all above taxa could drive sulfur reduction and make sulfur cycling complete.

Potential symbionts exist abundant in hypersaline environments

Abundant MAGs including 2 Ca. *Nanohaloarchaeota* MAGs and 2 Ca. *Woesearchaeota* MAGs in the DPANN superphylum, as well as 1 Ca. *Dependentiae* MAG and 1 Ca. *Nealsonbacteria* MAG in the CPR superphylum, were also observed in these saline-alkaline lakes, (Figs. 2 and 4). The metabolic potential of these microbes is typically limited because of the smaller genome size (Table S4). All six MAGs did not show the potential for dissimilatory sulfur or nitrogen metabolism (Fig. 4). Interestingly, most DPANN and CPR taxa are auxotrophic with respect to the biosynthesis of amino acids, purine and pyrimidine bases of nucleotides, and isoprenoids or fatty acids of the cell membrane (41). The two *Acholeplasmataceae* MAGs TB-1 and TB-2 were observed to be abundant in the sediment of HC27 (Fig. 4). *Acholeplasmataceae* is a class of cell-wall-free microbes (fried egg-like colony) that live together with plants or insects (42).

Members of the DPANN and CPR superphyla are known to have symbiotic lifestyles with other microbes (41, 43). We constructed a cooccurrence network based on the coverage of 385 MAGs in the 18 samples to predict the putative associated symbiont (Fig. 5). Four primary connected networks were identified, with fifteen separate networks having sparse MAGs. Only one abundant Ca. *Nanohaloarchaeota* MAG (NHA-1) was strongly co-present with the *Halobacteriaceae* MAG EA-19, while NHA-5 and NHA-3 were correlated with *Natronomonas* sp. EA-16 and the abundant *Halorubrum* sp. EA-5, as well as with each other (detailed shown in Fig. 5). The above results suggested that the putative symbiont of Ca. *Nanohaloarchaeota* is likely a member of the taxon *Halobacteria*.

Metabolic advantage of Ca. *Nanohaloarchaeota* in hypersaline environments

The presence of symbiont must make mutually beneficial relationship, otherwise the symbiont would be replaced by separate existence. We constructed the energy generation pathway in DPANN superphylum to deep understand the symbiotic lifestyle. DPANN and CPR cannot regenerate ATP via oxidative and photosynthetic phosphorylation due to the general absence of electron transport complexes and photosynthetic reaction center complexes (Table S6). Some taxa (especially NHA-1 and NHA-3) are believed to gain energy by substrate level phosphorylation via carbohydrate fermentation for the complete glycolysis pathway from hexose to pyruvate (Fig. 6a and b). Ca. *Woesearchaeota* in saline-alkaline lakes may ferment carbohydrates via a modified pathway or generate energy through another pathway considering the absence of 6-phosphofructose kinase (pfkAB or pfkC) (Fig. 6a and Table S6).

Pyruvate:ferredoxin oxidoreductase, alcohol dehydrogenase and lactate dehydrogenase were not detected in Ca. *Nanohaloarchaeota* MAGs (Table S6), indicating that pyruvate may be produced as final product for the symbiotic microbes (potentially *Halobacteria*). It was consistent that no *Halobacteria* MAGs contained polysaccharide phosphorylation pathway (Table S6). Pyruvate is considered to be a key nutrient in hypersaline environments (44), indicating that the Ca. *Nanohaloarchaeota* and Ca. *Woesearchaeota* taxa may function as primary degraders of polysaccharides (Fig. 6a)—at least in the symbiotic system.

Most DPANN MAGs contained alpha-amylase and glucose kinase, so that the 1,4-alpha-glucans (like starch) may be generally used as their carbon and energy sources (Fig. 6a). Interestingly, eight of twelve Ca. *Nanohaloarchaeota* MAGs had genes encoding glycogen phosphorylase (or named 1,4-alpha-glucan phosphorylase) and phosphomannomutase/phosphoglucomutase enzymes (Pgm), which catalyze the phosphorylation of polysaccharides and transfer glucose-1-phosphate to glucose-6-phosphate (Fig. 6b). In contrast, more Ca. *Woesearchaeota* MAGs encoded glycogen phosphorylase, but none of them harbored the *pgm* gene (Fig. 6a). More interestingly, the abundant MAG NHA-1 contained 1,4-alpha-glucans phosphorylase and complete glycolysis pathway, but not alpha-amylase (Fig. 6a). Because of more ATP produced compared with hydrolysis (Fig. 6c), we infer that 1,4-alpha-glucans phosphorylation may play a significant role in maintaining the symbiotic lifestyle between Ca. *Nanohaloarchaeota* sp. NHA-1 and its *Halobacteria* host (discuss below).

To estimate the importance of 1,4-alpha-glucans phosphorylation, we compared the similarity of functional genes among DPANN. In the phylogenomic tree, four separate clades in Ca. *Nanohaloarchaeota* were observed (Fig. 7a). The glycogen phosphorylase coding gene *pyg* was generally detected in clades II, III and IV but was not present in NHA-10 and NHA-12 from clade I (Fig. 6a). Among the separate clades, Pyg from different MAGs with a high similarity were located together (Fig. 7b), especially in NHA-1 and NHA-3. Interestingly, the amino acid sequences of the glycogen phosphorylase from clades II and III were located at closed branches, while that of clade IV was homologous with the enzyme from Ca. *Woesearchaeota* (Fig. 7b). The evolutional tree of Pyg indicated that phosphorylation was conserved in most taxa of Ca. *Nanohaloarchaeota*.

Discussion

In this study, a large variety of microorganisms were observed in both of the brine and sediment of the chloride-carbonate-sulfate lakes (Figs. 1 and 2, Table S4), from which a number of haloalkaliphilic microorganisms have been isolated (3, 7, 20). The pH value, carbonate/bicarbonate concentrations and salinity appear to be of importance in shaping the prokaryotic communities in salt lakes (45, 46). As shown in Fig. S2 and Fig. 1, the Cl^- concentration, which is positively correlated with pH, salinity, CO_3^{2-}, HCO_3^-, SO_4^{2-} and conductivity, was the key factor affecting microbial communities among these saline-alkaline lakes. Chloride and carbonate/bicarbonate, the primary anions and also major contributors to

osmotic pressure of the lakes (Table S1), determine the microbial community composition (26). The chloride-dominated brines have about twice the osmotic pressure of the carbonate-dominated brines with the same Na^+ molarity (20, 23), which explains why the chloride-dominated lakes had a larger influence on microbial community than the typical (bi)carbonate-rich soda lakes (8). The sediment environments exhibited a higher biodiversity when compared with the brine environments (Fig. S4a), as the sediment ecosystems, especially the anoxic environments, could provide more opportunities for niche diversification (23).

Interestingly, many elemental sulfur-reducing microbes, such as Halorubrum spp. EA-4, EA-5, Halarsenatibacter sp. FB-1, and Desulfonatronospira sp. DPB-1 (Fig. 4), were abundant under extremely hypersaline conditions, as the much lower concentrations of dissolved oxygen (47) and the notably reduced oxygen diffusion coefficients (48) boosted the anaerobic respiration of these microbes. In addition, diverse taxa were shown to be involved in sulfate and tetrathionate respiration (Table S6). With acetate as a substrate, the polysulfide/elemental sulfur reduction under alkaline conditions (pH 10) is much more exergonic (ΔG=-91.9 kJ/mol) than neutral pH conditions ($\Delta G^{0'}$= -6.6 kJ/mol) (Reaction 1 in Table 1), suggesting that this reaction is energetically more favorable for dissimilatory elemental sulfur reduction at a higher pH value (14). However, for those microbes utilizing heterotrophic and chemolithotrophic sulfate respirations, there are almost no differences in free energy changes between neutral and alkaline conditions. Given that polysulfide/elemental sulfur reducing microbes are able to obtain more free energy for ATP synthesis under alkaline conditions (Table 1), the difference in ATP yields between the two pH conditions could explain why polysulfide/elemental sulfur reducing microbes could gain a growth advantage in alkaline environments.

Table 1

Summary of Gibbs free energy change in sulfur reactions#

Rct. No.	Chemical reaction	$\Delta G^{0'}$ (kJ)	ΔG^0 at pH10 (kJ)	Ref.
1	$Acetate^- + 4S^0 + 4H_2O \lozenge 4HS^- + 2HCO_3^- + 5H^+$	-6.6	-91.9	(96)
2	$Acetate^- + 4S_4O_6^{2-} + 4H_2O \lozenge 2HCO_3^- + 9H^+ + 8S_2O_3^{2-}$	-233.4	-386.94	(49)
3	$Acetate^- + SO_4^{2-} \lozenge 2HCO_3^- + HS^-$	-47.3	-47.3	(49)
4	$4H_2 + SO_4^{2-} + H^+ \lozenge HS^- + 4H_2O$	-151.9	-134.84	(49)
# The ΔG values were calculated with acetate or hydrogen as samples, and exhibited the Gibbs free energy change per reaction. Eight electrons were transferred in every reaction.				

Alkaline lakes, including Soda-Saline lakes (Fig. 4) and typical soda lakes (13, 50), provide excess soluble phosphate and low toxic form of sulfide (HS^-), creating an advantage environment for the growth of diverse sulfur oxidizing microbes (20, 23). The sqr gene was found in an abundance of heterotrophic taxa, such as Actinobacteria, Chloroflexi, Alphaproteobacteria, Deltaproteobacteria, and Gammaproteobacteria, suggesting these microbes play a role in the detoxification of sulfide. In addition, some cyanobacteria have been reported to be anoxygenic photosynthetic bacteria and be capable of oxidizing sulfide by Sqr (51–54). The electrons obtained from sulfide oxidation are further transferred to the reducing equivalent NADPH via quinone and electron transport chain components, and are finally used for CO_2 fixation (52). Interestingly, a large number of strictly organotrophic microbes inhabiting soda lakes or marine environments are capable of oxidizing thiosulfate to tetrathionate or sulfate (35, 57). A higher growth rate of Limnobacter thiooxidans, a thiosulfate-oxidizing heterotrophic bacterium isolated from freshwater lake sediment, was observed by adding thiosulfate, suggesting that L. thiooxidans obtains energy advantage via the oxidation of thiosulfate (56). Heterotrophic sulfur-oxidizing microbes (HSOB) provided with thiosulfate restored the ATP synthesis in the starved cells (35), and increased the level of dark anaplerotic carbon dioxide assimilation (58, 59). Since ATP synthesis is a rate-limiting step for the anaplerotic CO_2 assimilation, the energy advantage obtained from sulfide oxidation by Sqr could be a reasonable explanation for the high coverage of Sqr-containing heterotrophs.

Ca. Nanohaloarchaeota and other DPANN members are difficult to culture in the laboratory (43, 61, 62), as their small sizes of genomes limit their anabolic abilities (41, 63). Generally, these microbes still need to uptake nutrients from their symbionts for the biosynthesis of nucleic acids, proteins and lipids. Ca. Nanohaloarchaeum antarcticus was isolated together with Halorubrum lacusprofundi but away from other species (43). The growth of Ca. Nanohaloarchaeota is probably dependent on a specific Halobacteria host (43) (Fig. 5), increasing the difficulty of culturing Ca. Nanohaloarchaeota. Although few Ca. Nanohaloarchaeota species have been co-cultured with their hosts, they have been detected to be abundant in multiple hypersaline environments, including neutral salterns (63, 64), soda lakes (22), and Soda-Saline lakes (Figs. 2 and 4). The “salt in” strategy Ca. Nanohaloarchaeota employs to resists osmotic force (22), provides an effective solution of saving energy in hypersaline environments (26, 28). This energy-saving mechanism may contribute to the observed high abundance of Ca. Nanohaloarchaeota in hypersaline environments. In addition, Ca. Nanohaloarchaeota is able to utilize polysaccharide, and generate ATP by substrate level phosphorylation during glycolysis (22, 41). Alpha-amylase could be responsible for the hydrolysis of polysaccharide (22, 41, 62). More recently, Ca. Nanahalobium has been proven to be capable of hydrolyzing alpha-glucans (65). Amylase genes were found to be widely distributed in Ca. Nanohaloarchaeota and Ca. Woesearchaeota (Fig. 6a), but they are absent in NHA-1, the most abundant Ca. Nanohaloarchaeota strain in hypersaline environments. The 1,4-alpha-glucan phosphorylation pathway, which is participated in maltose/maltodextrin/glycogen metabolism in both archaea and bacteria (66–68), could be employed by NHA-1 strain as an alternative strategy for polysaccharide degradation (Fig. 6a and b). However, both 4-alpha-glucanotransferase catalyzing the conversion of maltose to maltodextrin and glycogen synthase responsible for the synthesis of glycogen were not available in NHA-1 (Table S6). Therefore we hypothesize that extracellular

maltodextrin is a putative substrate. One less ATP molecule is used when one glucoside molecule is degraded via phosphorylation pathway rather than hydrolysis pathway, so one more ATP molecule will be made by using maltodextrin substrate (Fig. 6c). This relatively more efficient ATP generation system present in Ca. Nanohaloarchaeota MAG may provide the symbionts with a growth advantage in the competition with the free-living Halobacteria, which typically utilize starch via the alpha-amylase based hydrolysis pathway (69).

Conclusions

The chloride-carbonate-sulfate lakes (also called Soda-Saline lakes) are double-extreme ecological environments with high pH and high salinity values, and the diversity of metabolic process that functioned well in such environments remains to be systematically investigated. The microbial composition and their metabolic potential in the brines and sediments of two chloride-carbonate-sulfate lakes were analyzed. The microbiomes from different habitats were composed of few abundant and numerous rare taxa. These abundant taxa represented most branches of the phylogenomic tree. The oxidation and reduction of sulfur and polysaccharide phosphorylation existed in certain abundant taxa, that may increase the adaptation to extreme alkaline and saline environments, and we discuss the superiority of them in terms of energy production and thermodynamics. RSCs could be utilized as a putative accessory energy source for heterotrophs under nutrient limited conditions. Elemental sulfur respiration was easier to occur under high pH may because of thermodynamic advantages, and that was in favor of this type of sulfur reduction microbes in a high abundance. More energy was produced by phosphorylation pathway of 1,4-alpha-glucans compared with hydrolysis. The above results provide novel insights into the diverse lifestyles and adaptive characterizations of the prokaryotes thriving in such double-extreme environments.

Methods

Physicochemical characterization

Salinity was measured by refractometry using a handheld refractometer (Beijing Wanchengbeizeng Precision Instrument Co., Ltd., Beijing, China). Conductivity, pH and the concentrations of CO_3^{2-} and HCO_3^- were measured using a SensoDirect 150 and an MD600 Photometer (Lovibond® Water Testing, Dortmund, Germany). The concentrations of other inorganic ions (Cl^-, SO_4^{2-}, PO_4^{3-}, Mg^{2+}, Ca^{2+}, and NH_4^+) and total organic nitrogen were measured using an Aquakem™ 250 discrete photometric autoanalyzer (Thermo Fisher Scientific, MA, USA).

DNA extraction and metagenomic sequencing

Brine samples were prefiltered through four layers of gauze to eliminate eukaryotic animals and plants. The microorganisms in each sample were collected by 0.8- and 0.22-μm filters. Then, the filters were used to extract DNA with a PowerWater® DNA Isolation kit (MoBio, CA, USA). DNA extracted from the same sample was mixed as a single sample. Total DNA of sediment samples was extracted using a PowerSoil® DNA Isolation kit (MoBio, CA, USA). The DNA concentration and purity were measured using a Qubit® dsDNA Assay kit with a Qubit®2.0 Fluorometer (Life Technologies, CA, USA) and a NanoPhotometer® spectrophotometer (IMPLEN, CA, USA), respectively. The OD_{260}/OD_{280} values of the samples were between 1.8~2.0, and DNA concentrations were >1 μg. Library construction and shotgun sequencing were performed using an Illumina HiSeq-2000 platform (Illumina, USA) to generate 150-bp paired-end reads.

Metagenomic data analysis based on a nonredundant gene catalog

Quality control of the raw reads was conducted using Readfq (V8, https://github.com/cjfields/readfq) to filter out low-quality reads and ensure that each read had (a) no more than 40 bases with a quality score smaller than 38, (b) less than 10 ambiguous nucleotides in one read, and (c) no reads sharing more than a 15-bp overlap with the adapter. Clean reads were assembled into contigs using MEGAHIT (v1.1.2) (70) with the following parameters: –presets meta-large (-min-count 2 –k-min 27 –k-max 127 –k-step 10). Unassembled read pairs were retrieved by mapping paired-reads to contigs using BBMap (v37.57) (https://sourceforge.net/projects/bbmap/) with the following parameters: kfilter=22 subfilter=15 maxindel=80. Coassembly was conducted using MEGAHIT with the same parameters described above to acquire low-abundance reads. Contigs from single-assembled samples and one coassembly were merged together, and contigs with <500 bp were removed (71).

Open reading frames (ORFs) were predicted using MetaGeneMark (GeneMark.hmm v3.38) (72) with the default parameters. ORFs with lengths <100 bp were removed to reduce the number of pseudogenes (71). Redundancy removal was executed using CD-HIT (v4.7) (73) with the following parameters: -c 0.95 -G 0 -aS 0.9 -g 1 -d 0. Clean reads from the 18 samples were mapped to the nr-ORF catalog using BWA mem (v0.7.17) (74) with the default parameters. ORFs with <2 reads aligned from the 18 samples were removed to prevent incorrect assembly. The abundance of each nonredundant gene in one sample was calculated based on the proportion of the mapped number of reads (counted by BamM: http://ecogenomics.github.io/BamM) divided by the gene length (75). Taxonomy assignments were performed by mapping the amino acid sequences against the NCBI nonredundant database (Version: 20170923, https://www.ncbi.nlm.nih.gov/) using Diamond (v0.9.10.111) (76) with the following parameters: –taxonmap –taxonnodes -e 1e-5 –top 10. Nonredundant genes were assigned to the corresponding taxa calculated by the Lowest Common Ancestor (LCA) algorithm (77) in Diamond. The abundance of each metagenomic operational taxonomic unit (mOTU) (78) was the sum of the abundances of all nonredundant genes assigned to that mOTU (75), and was supplied in Additional file 3. Functional annotation was performed using the KEGG databases by uploading to the Automatic

Annotation Server (v2.1) (79), where the GENES dataset was set for Prokaryotes, while the Assignment method was set as BBH.

Binning and post analysis of MAGs

Contigs were binned using MetaBAT (v2.12.1) (80) based on their tetranucleotide frequency and differential coverage values obtained by mapping the clean data onto the contig dataset using BWA mem (v0.7.17) (74). Genome completeness was estimated using CheckM (v1.0.12) (81) to generate high-quality genomes with >90% completeness and <10% contamination, 80-90% completeness and <5% contamination, or 50-80% completeness and <2% contamination (82). Draft genomes were dereplicated according to ANI using dRep (v2.2.1) (83). Gene and protein-coding sequences were predicted using Prodigal (v2.6.3) (84). The abundance of each MAG in each sample was calculated, equaling the sum of all contigs coverage multiply their own lengths divided by genome size. Taxonomic assignments for each bin were performed using CheckM, the Diamond aligned to UniProt TrEMBL database (85), and PhyloPhlan (v0.99) (86) and were manually curated afterwards. A phylogenomic tree was constructed using reference genomes based on the most conserved 400 proteins across bacteria and archaea using PhyloPhlan and visualized using iTOL (v4) (87). Functional annotation was conducted using GhostKOALA ('genus_prokaryotes+family_eukaryotes+viruses'; v2.0) (88) to reconstruct the metabolic pathways, and was supplied in Additional file 5. The direction of dissimilatory sulfur metabolism by DsrAB was determined by the present or absent of *dsrD* and *dsrEFH* (89), and these genes were predicted with HMM profile from TIGRFAM (90) and Pfam (91) using Hmmscan v3.1b2 (92). For the phylogenetic analysis, proteins assigned to *Nanohaloarchaeota* and *Woesearchaeota* were retrieved from the corresponding 19 MAGs and aligned using MEGA X (93) with the reference protein alpha-glucan phosphorylase from *Escherichia* coli (PWL89129.1).

Statistical analysis

The datasets generated above were statistically analyzed using the free software R Project (https://www.r-project.org/). The sampling map was visualized using the leaflet package. The Shannon diversity indexes of samples were calculated using the vegan package (http://vegan.r-forge.r-project.org/) and visualized by the ggpubr package (https://CRAN.R-project.org/package=ggpubr). Heatmap cluster analysis and principal component analysis (PCA) were visualized using the pheatmap (https://CRAN.R-project.org/package=pheatmap) and ggbiplot packages (https://github.com/vqv/ggbiplot), respectively. Redundancy analysis (RDA) was performed using the vegan package with all taxon abundances in genus level and physiochemical data. The cooccurrence network was based on the abundances of 385 MAGs across 18 samples (Table S5). Pearson correlation coefficients were calculated using the psych package (https://CRAN.R-project.org/package=psych), where a Pearson correlation coefficient > 0.9 and p value < 0.01 were used. The network was visualized using Cytoscape (94).

Declarations

Ethics approval and consent to participate

Not applicable

Consent for publication

Not applicable

Availability of data and materials

The raw sequence reads of 18 metagenomes have been deposited in NCBI (https://www.ncbi.nlm.nih.gov/), with the projectID PRJNA549802, and in gcMeta (95), with the projectID NMDC10010899. The binning results can be accessed through the ftp site ftp://bio-mirror.im.ac.cn/public_data/saltlake_genome_bins/.

Competing interests

The authors declare that they have no competing interests.

Funding

This study was funded by the National Natural Science Foundation of China (grant number 91751201) and was partially supported by the National Science and Technology Foundation Project of China (grant numbers 2015FY110100 and 2017FY100300).

Authors' contributions

HX designed and supervised the study. DZ, SZ, QX, JC, JZ, FC, and HX collected water and sediment samples. QX and JC measured physicochemical characteristics. YZ extracted DNA from environmental samples. DZ and SZ performed bioinformatic and statistical analyses under the partial supervision of HY and SH. DZ and SZ prepared the figures and wrote the manuscript under the guidance of HX. ML, YZ, SL, and SH participated in the discussion and revision. All authors read and approved the final manuscript.

Acknowledgments

We thank Dr. Wenyu Shi for data submission to NCBI and gcMeta.

Authors' information

[1]State Key Laboratory of Microbial Resources, Institute of Microbiology, Chinese Academy of Sciences, Beijing, China; [2]College of Life Sciences, University of Chinese Academy of Sciences, Beijing, China; [3]Beijing Institute of Genomics, Chinese Academy of Sciences, Beijing, China.

References

1. Grant WD, Sorokin DY. Distribution and diversity of soda lake alkaliphiles. In: Horikoshi K, editor. Extremophiles Handbook. Tokyo: Springer Japan; 2011. p. 27-54.
2. Lanzen A, Simachew A, Gessesse A, Chmolowska D, Jonassen I, Ovreas L. Surprising prokaryotic and eukaryotic diversity, community structure and biogeography of Ethiopian soda lakes. Plos One. 2013;8(8).
3. Grant WD. Alkaline environments and biodiversity. In: Gerday C, Glansdorff N, editors. Extremophiles Handbook. UK: Eolss; 2006.
4. Mesbah NM, Abou-El-Ela SH, Wiegel J. Novel and unexpected prokaryotic diversity in water and sediments of the alkaline, hypersaline lakes of the wadi an natrun, egypt. Microb Ecol. 2007;54(4):598-617.
5. Asao M, Pinkart HC, Madigan MT. Diversity of extremophilic purple phototrophic bacteria in Soap Lake, a central Washington (USA) soda lake. Environ Microbiol. 2011;13(8):2146-57.
6. Kompantseva EI, Komova AV, Rusanov II, Pimenov NV, Sorokin DY. Primary production of organic matter and phototrophic communities in the soda lakes of the Kulunda Steppe (Altai Krai). Microbiology+. 2009;78(5):643-9.
7. Antony CP, Kumaresan D, Hunger S, Drake HL, Murrell JC, Shouche YS. Microbiology of Lonar Lake and other soda lakes. Isme J. 2013;7(3):468-76.
8. Zorz JK, Sharp C, Kleiner M, Gordon PMK, Pon RT, Dong X, et al. A shared core microbiome in soda lakes separated by large distances. Nat Commun. 2019;10(1):4230.
9. Melack JM, Kilham P. Photosynthetic Rates of Phytoplankton in East-African Alkaline, Saline Lakes. Limnol Oceanogr. 1974;19(5):743-55.

10. Melack JM. Photosynthetic activity of phytoplankton in tropical African soda lakes. Hydrobiologia. 1981;81-2(Jun):71-85.
11. Vavourakis CD, Mehrshad M, Balkema C, van Hall R, Andrei AS, Ghai R, et al. Metagenomes and metatranscriptomes shed new light on the microbial-mediated sulfur cycle in a Siberian soda lake. BMC biology. 2019;17(1):69.
12. Sorokin DY, Kuenen JG, Muyzer G. The microbial sulfur cycle at extremely haloalkaline conditions of soda lakes. Front Microbiol. 2011;2.
13. Tourova TP, Slobodova NV, Bumazhkin BK, Kolganova TV, Muyzer G, Sorokin DY. Analysis of community composition of sulfur-oxidizing bacteria in hypersaline and soda lakes using soxB as a functional molecular marker. Fems Microbiol Ecol. 2013;84(2):280-9.
14. Sorokin DY, Rusanov II, Pimenov NV, Tourova TP, Abbas B, Muyzer G. Sulfidogenesis under extremely haloalkaline conditions in soda lakes of Kulunda Steppe (Altai, Russia). Fems Microbiol Ecol. 2010;73(2):278-90.
15. Stam MC, Mason PRD, Pallud C, Van Cappellen P. Sulfate reducing activity and sulfur isotope fractionation by natural microbial communities in sediments of a hypersaline soda lake (Mono Lake, California). Chem Geol. 2010;278(1-2):23-30.
16. Oremland RS, Saltikov CW, Stolz JF, Hollibaugh JT. Autotrophic microbial arsenotrophy in arsenic-rich soda lakes. Fems Microbiol Lett. 2017;364(15).
17. Iversen N, Oremland RS, Klug MJ. Big Soda Lake (Nevada) .3. Pelagic Methanogenesis and Anaerobic Methane Oxidation. Limnol Oceanogr. 1987;32(4):804-14.
18. Carini SA, Joye SB. Nitrification in Mono Lake, California: Activity and community composition during contrasting hydrological regimes. Limnol Oceanogr. 2008;53(6):2546-57.
19. Phitsuwan P, Morais S, Dassa B, Henrissat B, Bayer EA. The Cellulosome Paradigm in An Extreme Alkaline Environment. Microorganisms. 2019;7(9).
20. Sorokin DY, Banciu HL, Muyzer G. Functional microbiology of soda lakes. Curr Opin Microbiol. 2015;25:88-96.
21. Sorokin DY, Berben T, Melton ED, Overmars L, Vavourakis CD, Muyzer G. Microbial diversity and biogeochemical cycling in soda lakes. Extremophiles. 2014;18(5):791-809.
22. Vavourakis CD, Ghai R, Rodriguez-Valera F, Sorokin DY, Tringe SG, Hugenholtz P, et al. Metagenomic insights into the uncultured diversity and physiology of microbes in four hypersaline soda lake brines. Front Microbiol. 2016;7.
23. Vavourakis CD, Andrei AS, Mehrshad M, Ghai R, Sorokin DY, Muyzer G. A metagenomics roadmap to the uncultured genome diversity in hypersaline soda lake sediments. Microbiome. 2018;6.
24. Kovaleva OL, Tourova TP, Muyzer G, Kolganova TV, Sorokin DY. Diversity of RuBisCO and ATP citrate lyase genes in soda lake sediments. Fems Microbiol Ecol. 2011;75(1):37-47.
25. Tourova TP, Kovaleva OL, Bumazhkin BK, Patutina EO, Kuznetsov BB, Bryantseva IA, et al. Application of Ribulose-1,5-Bisphosphate Carboxylase/Oxygenase Genes as Molecular Markers for Assessment

of the Diversity of Autotrophic Microbial Communities Inhabiting the Upper Sediment Horizons of the Saline and Soda Lakes of the Kulunda Steppe. Microbiology+. 2011;80(6):812-25.

26. Banciu HL, Muntyan MS. Adaptive strategies in the double-extremophilic prokaryotes inhabiting soda lakes. Curr Opin Microbiol. 2015;25:73-9.
27. Roberts MF. Organic compatible solutes of halotolerant and halophilic microorganisms. Saline systems. 2005;1:5.
28. Gunde-Cimerman N, Plemenitas A, Oren A. Strategies of adaptation of microorganisms of the three domains of life to high salt concentrations. FEMS microbiology reviews. 2018.
29. Krulwich TA, Sachs G, Padan E. Molecular aspects of bacterial pH sensing and homeostasis. Nature reviews Microbiology. 2011;9(5):330-43.
30. Zheng XZ, Minggang; Xu, Chang; Li, Bingxiao. Salt lake records of China. 2002. (in Chinese).
31. Boros E, Kolpakova M. A review of the defining chemical properties of soda lakes and pans: An assessment on a large geographic scale of Eurasian inland saline surface waters. Plos One. 2018;13(8).
32. Leon MJ, Fernandez AB, Ghai R, Sanchez-Porro C, Rodriguez-Valera F, Ventosa A. From Metagenomics to Pure Culture: Isolation and Characterization of the Moderately Halophilic Bacterium Spiribacter salinus gen. nov., sp nov. Appl Environ Microb. 2014;80(13):3850-7.
33. Lopez-Perez M, Ghai R, Leon MJ, Rodriguez-Olmos A, Copa-Patino JL, Soliveri J, et al. Genomes of "Spiribacter", a streamlined, successful halophilic bacterium. Bmc Genomics. 2013;14.
34. Klatt JM, Haas S, Yilmaz P, de Beer D, Polerecky L. Hydrogen sulfide can inhibit and enhance oxygenic photosynthesis in a cyanobacterium from sulfidic springs. Environ Microbiol. 2015;17(9):3301-13.
35. Sorokin DY. Oxidation of inorganic sulfur compounds by obligately organotrophic bacteria. Microbiology+. 2003;72(6):641-53.
36. Sorokin DY, Chernyh NA. Desulfonatronospira sulfatiphila sp nov., and Desulfitispora elongata sp nov., two novel haloalkaliphilic sulfidogenic bacteria from soda lakes. Int J Syst Evol Micr. 2017;67(2):396-401.
37. Sorokin DY, Tourova TP, Henstra AM, Stams AJM, Galinski EA, Muyzer G. Sulfidogenesis under extremely haloalkaline conditions by Desulfonatronospira thiodismutans gen. nov., sp nov., and Desulfonatronospira delicata sp nov - a novel lineage of Deltaproteobacteria from hypersaline soda lakes. Microbiol-Sgm. 2008;154:1444-53.
38. Sorokin DY, Tourova TP, Mussmann M, Muyzer G. Dethiobacter alkaliphilus gen. nov sp nov., and Desulfurivibrio alkaliphilus gen. nov sp nov.: two novel representatives of reductive sulfur cycle from soda lakes. Extremophiles. 2008;12(3):431-9.
39. Lien T, Madsen M, Steen IH, Gjerdevik K. Desulfobulbus rhabdoformis sp. nov., a sulfate reducer from a water-oil separation system. Int J Syst Bacteriol. 1998;48:469-74.

40. Pikuta EV, Hoover RB, Bej AK, Marsic D, Whitman WB, Cleland D, et al. Desulfonatronum thiodismutans sp nov., a novel alkaliphilic, sulfate-reducing bacterium capable of lithoautotrophic growth. Int J Syst Evol Micr. 2003;53:1327-32.
41. Castelle CJ, Brown CT, Anantharaman K, Probst AJ, Huang RH, Banfield JF. Biosynthetic capacity, metabolic variety and unusual biology in the CPR and DPANN radiations. Nature reviews Microbiology. 2018;16(10):629-45.
42. Freundt EA, Whitcomb RF, Barile MF, Razin S, Tully JG. Proposal for Elevation of the Family Acholeplasmataceae to Ordinal Rank - Acholeplasmatales. Int J Syst Bacteriol. 1984;34(3):346-9.
43. Hamm JN, Erdmann S, Eloe-Fadrosh EA, Angeloni A, Zhong L, Brownlee C, et al. Unexpected host dependency of Antarctic Nanohaloarchaeota. P Natl Acad Sci USA. 2019;116(29):14661-70.
44. Oren A. Pyruvate: A key Nutrient in Hypersaline Environments? Microorganisms. 2015;3(3):407-16.
45. Pagaling E, Wang HZ, Venables M, Wallace A, Grant WD, Cowan DA, et al. Microbial biogeography of six salt lakes in Inner Mongolia, China, and a salt lake in Argentina. Appl Environ Microb. 2009;75(18):5750-60.
46. Simachew A, Lanzen A, Gessesse A, Ovreas L. Prokaryotic community diversity along an increasing salt gradient in a soda ash concentration pond. Microb Ecol. 2016;71(2):326-38.
47. Sherwood JE, Stagnitti F, Kokkinn MJ, Williams WD. Dissolved-Oxygen Concentrations in Hypersaline Waters. Limnol Oceanogr. 1991;36(2):235-50.
48. Jamnongwong M, Loubiere K, Dietrich N, Hebrard G. Experimental study of oxygen diffusion coefficients in clean water containing salt, glucose or surfactant: Consequences on the liquid-side mass transfer coefficients. Chem Eng J. 2010;165(3):758-68.
49. Thauer RK, Jungermann K, Decker K. Energy conservation in chemotrophic anaerobic bacteria. Bacteriological reviews. 1977;41(1):100-80.
50. Sorokin DY, Kuenen JG. Haloalkaliphilic sulfur-oxidizing bacteria in soda lakes. FEMS microbiology reviews. 2005;29(4):685-702.
51. Sybesma C, Schowanek D, Slooten L, Walravens N. Anoxygenic Photosynthetic Hydrogen-Production and Electron-Transport in the Cyanobacterium Oscillatoria-Limnetica. Photosynth Res. 1986;9(1-2):149-58.
52. Hamilton TL, Klatt JM, de Beer D, Macalady JL. Cyanobacterial photosynthesis under sulfidic conditions: insights from the isolate Leptolyngbya sp. strain hensonii. Isme J. 2018;12(2):568-84.
53. Grim SL, Dick GJ. Photosynthetic versatility in the genome of Geitlerinema sp. PCC 9228 (formerly Oscillatoria limnetica 'Solar Lake'), a model anoxygenic photosynthetic cyanobacterium. Front Microbiol. 2016;7.
54. Cohen Y, Jorgensen BB, Padan E, Shilo M. Sulfide-Dependent Anoxygenic Photosynthesis in Cyanobacterium Oscillatoria-Limnetica. Nature. 1975;257(5526):489-92.
55. Shibata H, Kobayashi S. Sulfide oxidation in gram-negative bacteria by expression of the sulfide-quinone reductase gene of Rhodobacter capsulatus and by electron transport to ubiquinone. Can J

Microbiol. 2001;47(9):855-60.
56. Spring S, Kampfer P, Schleifer KH. Limnobacter thiooxidans gen. nov., sp nov., a novel thiosulfate-oxidizing bacterium isolated from freshwater lake sediment. Int J Syst Evol Micr. 2001;51:1463-70.
57. Sorokin DY, Tourova TP, Muyzer G. Oxidation of thiosulfate to tetrathionate by an haloarchaeon isolated from hypersaline habitat. Extremophiles. 2005;9(6):501-4.
58. Perez RC, Matin A. Carbon dioxide assimilation by Thiobacillus novellus under nutrient-limited mixotrophic conditions. J Bacteriol. 1982;150(1):46-51.
59. Tuttle JH, Jannasch HW. Thiosulfate stimulation of microbial dark assimilation of carbon dioxide in shallow marine waters. Microb Ecol. 1977;4(1):9-25.
60. Sorokin DY, Messina E, Smedile F, Roman P, Damste JSS, Ciordia S, et al. Discovery of anaerobic lithoheterotrophic haloarchaea, ubiquitous in hypersaline habitats. Isme J. 2017;11(5):1245-60.
61. Castelle CJ, Banfield JF. Major New Microbial Groups Expand Diversity and Alter our Understanding of the Tree of Life. Cell. 2018;172(6):1181-97.
62. Liu XB, Li M, Castelle CJ, Probst AI, Zhou ZC, Pan J, et al. Insights into the ecology, evolution, and metabolism of the widespread Woesearchaeotal lineages. Microbiome. 2018;6.
63. Narasingarao P, Podell S, Ugalde JA, Brochier-Armanet C, Emerson JB, Brocks JJ, et al. De novo metagenomic assembly reveals abundant novel major lineage of Archaea in hypersaline microbial communities. Isme J. 2012;6(1):81-93.
64. Ghai R, Pasic L, Fernandez AB, Martin-Cuadrado AB, Mizuno CM, McMahon KD, et al. New Abundant Microbial Groups in Aquatic Hypersaline Environments. Sci Rep-Uk. 2011;1.
65. La Cono V, Messina E, Rohde M, Arcadi E, Ciordia S, Crisafi F, et al. Differential polysaccharide utilization is the basis for a nanohaloarchaeon : haloarchaeon symbiosis. bioRxiv. 2019:794461.
66. Xavier KB, Peist R, Kossmann M, Boos W, Santos H. Maltose metabolism in the hyperthermophilic archaeon Thermococcus litoralis: Purification and characterization of key enzymes. J Bacteriol. 1999;181(11):3358-67.
67. Boos W, Shuman H. Maltose/maltodextrin system of Escherichia coli: Transport, metabolism, and regulation. Microbiol Mol Biol R. 1998;62(1):204-+.
68. Seibold GM, Wurst M, Eikmanns BJ. Roles of maltodextrin and glycogen phosphorylases in maltose utilization and glycogen metabolism in Corynebacterium glutamicum. Microbiol-Sgm. 2009;155:347-58.
69. Perez-Pomares F, Bautista V, Ferrer J, Pire C, Marhuenda-Egea FC, Bonete MJ. alpha-amylase activity from the halophilic archaeon Haloferax mediterranei. Extremophiles. 2003;7(4):299-306.
70. Li DH, Liu CM, Luo RB, Sadakane K, Lam TW. MEGAHIT: an ultra-fast single-node solution for large and complex metagenomics assembly via succinct de Bruijn graph. Bioinformatics. 2015;31(10):1674-6.
71. Qin N, Yang FL, Li A, Prifti E, Chen YF, Shao L, et al. Alterations of the human gut microbiome in liver cirrhosis. Nature. 2014;513(7516):59-+.

72. Zhu WH, Lomsadze A, Borodovsky M. Ab initio gene identification in metagenomic sequences. Nucleic Acids Res. 2010;38(12).
73. Li W, Godzik A. Cd-hit: a fast program for clustering and comparing large sets of protein or nucleotide sequences. Bioinformatics. 2006;22(13):1658-9.
74. Li H, Durbin R. Fast and accurate long-read alignment with Burrows-Wheeler transform. Bioinformatics. 2010;26(5):589-95.
75. Qin J, Li Y, Cai Z, Li S, Zhu J, Zhang F, et al. A metagenome-wide association study of gut microbiota in type 2 diabetes. Nature. 2012;490(7418):55-60.
76. Buchfink B, Xie C, Huson DH. Fast and sensitive protein alignment using DIAMOND. Nat Methods. 2015;12(1):59-60.
77. Huson DH, Auch AF, Qi J, Schuster SC. MEGAN analysis of metagenomic data. Genome Res. 2007;17(3):377-86.
78. Sunagawa S, Mende DR, Zeller G, Izquierdo-Carrasco F, Berger SA, Kultima JR, et al. Metagenomic species profiling using universal phylogenetic marker genes. Nat Methods. 2013;10(12):1196-+.
79. Moriya Y, Itoh M, Okuda S, Yoshizawa AC, Kanehisa M. KAAS: an automatic genome annotation and pathway reconstruction server. Nucleic Acids Res. 2007;35:W182-W5.
80. Kang DD, Froula J, Egan R, Wang Z. MetaBAT, an efficient tool for accurately reconstructing single genomes from complex microbial communities. Peerj. 2015;3:e1165.
81. Parks DH, Imelfort M, Skennerton CT, Hugenholtz P, Tyson GW. CheckM: assessing the quality of microbial genomes recovered from isolates, single cells, and metagenomes. Genome Res. 2015;25(7):1043-55.
82. Tully BJ, Graham ED, Heidelberg JF. The reconstruction of 2,631 draft metagenome-assembled genomes from the global oceans. Sci Data. 2018;5.
83. Olm MR, Brown CT, Brooks B, Banfield JF. dRep: a tool for fast and accurate genomic comparisons that enables improved genome recovery from metagenomes through de-replication. Isme J. 2017;11(12):2864-8.
84. Hyatt D, Chen GL, LoCascio PF, Land ML, Larimer FW, Hauser LJ. Prodigal: prokaryotic gene recognition and translation initiation site identification. Bmc Bioinformatics. 2010;11.
85. Bateman A, Martin MJ, O'Donovan C, Magrane M, Alpi E, Antunes R, et al. UniProt: the universal protein knowledgebase. Nucleic Acids Res. 2017;45(D1):D158-D69.
86. Segata N, Bornigen D, Morgan XC, Huttenhower C. PhyloPhlAn is a new method for improved phylogenetic and taxonomic placement of microbes. Nat Commun. 2013;4.
87. Letunic I, Bork P. Interactive Tree Of Life (iTOL) v4: recent updates and new developments. Nucleic Acids Res. 2019.
88. Kanehisa M, Sato Y, Morishima K. BlastKOALA and GhostKOALA: KEGG Tools for Functional Characterization of Genome and Metagenome Sequences. Journal of molecular biology. 2016;428(4):726-31.

89. Anantharaman K, Hausmann B, Jungbluth SP, Kantor RS, Lavy A, Warren LA, et al. Expanded diversity of microbial groups that shape the dissimilatory sulfur cycle. Isme J. 2018;12(7):1715-28.
90. Haft DH, Selengut JD, White O. The TIGRFAMs database of protein families. Nucleic Acids Res. 2003;31(1):371-3.
91. El-Gebali S, Mistry J, Bateman A, Eddy SR, Luciani A, Potter SC, et al. The Pfam protein families database in 2019. Nucleic Acids Res. 2019;47(D1):D427-D32.
92. Eddy SR. Accelerated Profile HMM Searches. Plos Comput Biol. 2011;7(10).
93. Kumar S, Stecher G, Li M, Knyaz C, Tamura K. MEGA X: Molecular Evolutionary Genetics Analysis across Computing Platforms. Mol Biol Evol. 2018;35(6):1547-9.
94. Shannon P, Markiel A, Ozier O, Baliga NS, Wang JT, Ramage D, et al. Cytoscape: A software environment for integrated models of biomolecular interaction networks. Genome Res. 2003;13(11):2498-504.
95. Shi WY, Qi HY, Sun QL, Fan GM, Liu SJ, Wang J, et al. gcMeta: a Global Catalogue of Metagenomics platform to support the archiving, standardization and analysis of microbiome data. Nucleic Acids Res. 2019;47(D1):D637-D48.
96. Oren A. Thermodynamic limits to microbial life at high salt concentrations. Environ Microbiol. 2011;13(8):1908-23.

Figures

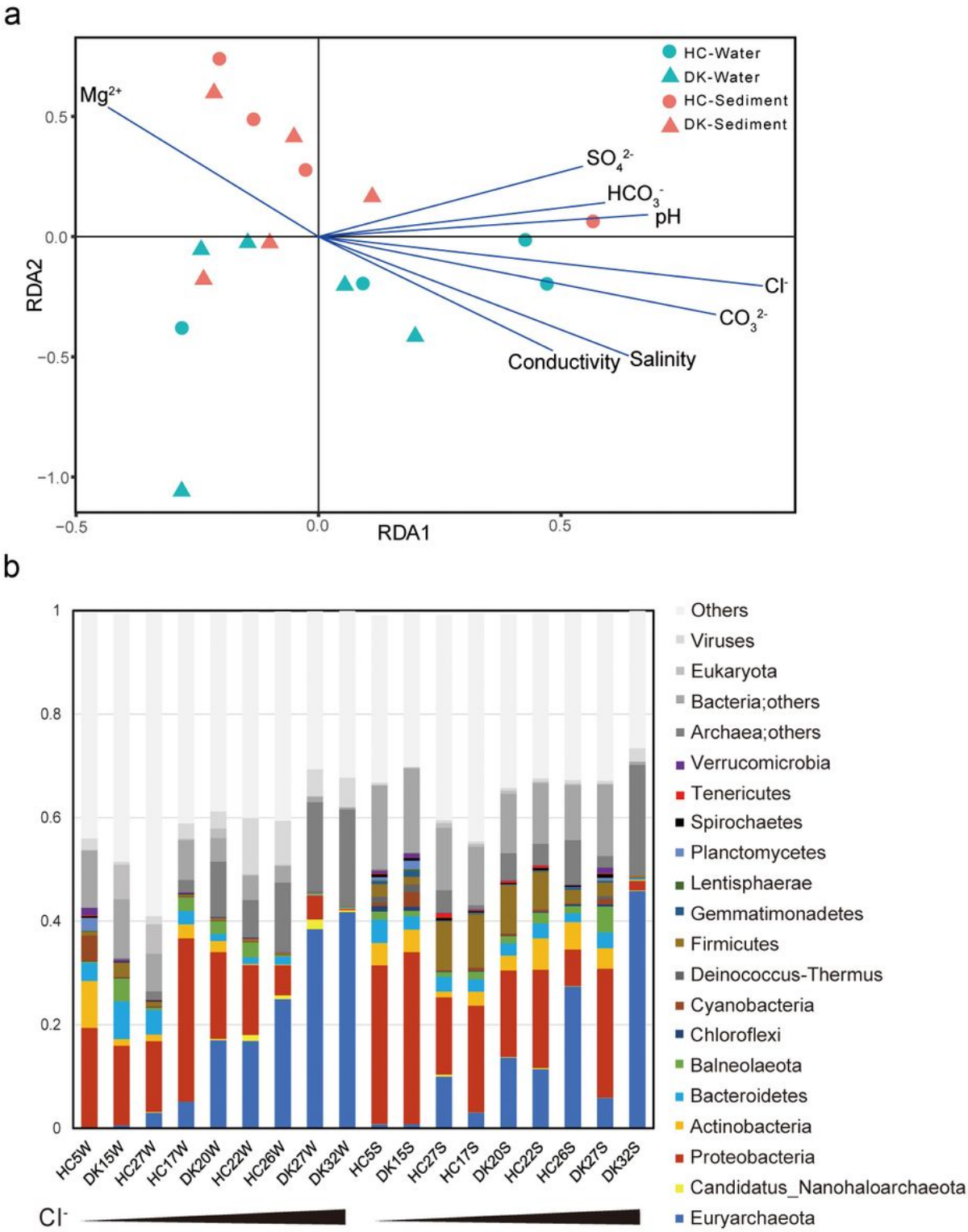

Figure 1

The relationship between environmental factors and microbial communities. a. The influence of environmental factors on microbial community structure was analyzed by redundancy analysis. b. The microbial composition of eighteen samples and the observed relative abundances (Table S3) of taxa at the phylum level. The total relative abundances of taxa (greater than 0.1%) are shown. The first nine

samples were water samples, while the last nine were sediment samples and were sorted by Cl- concentration.

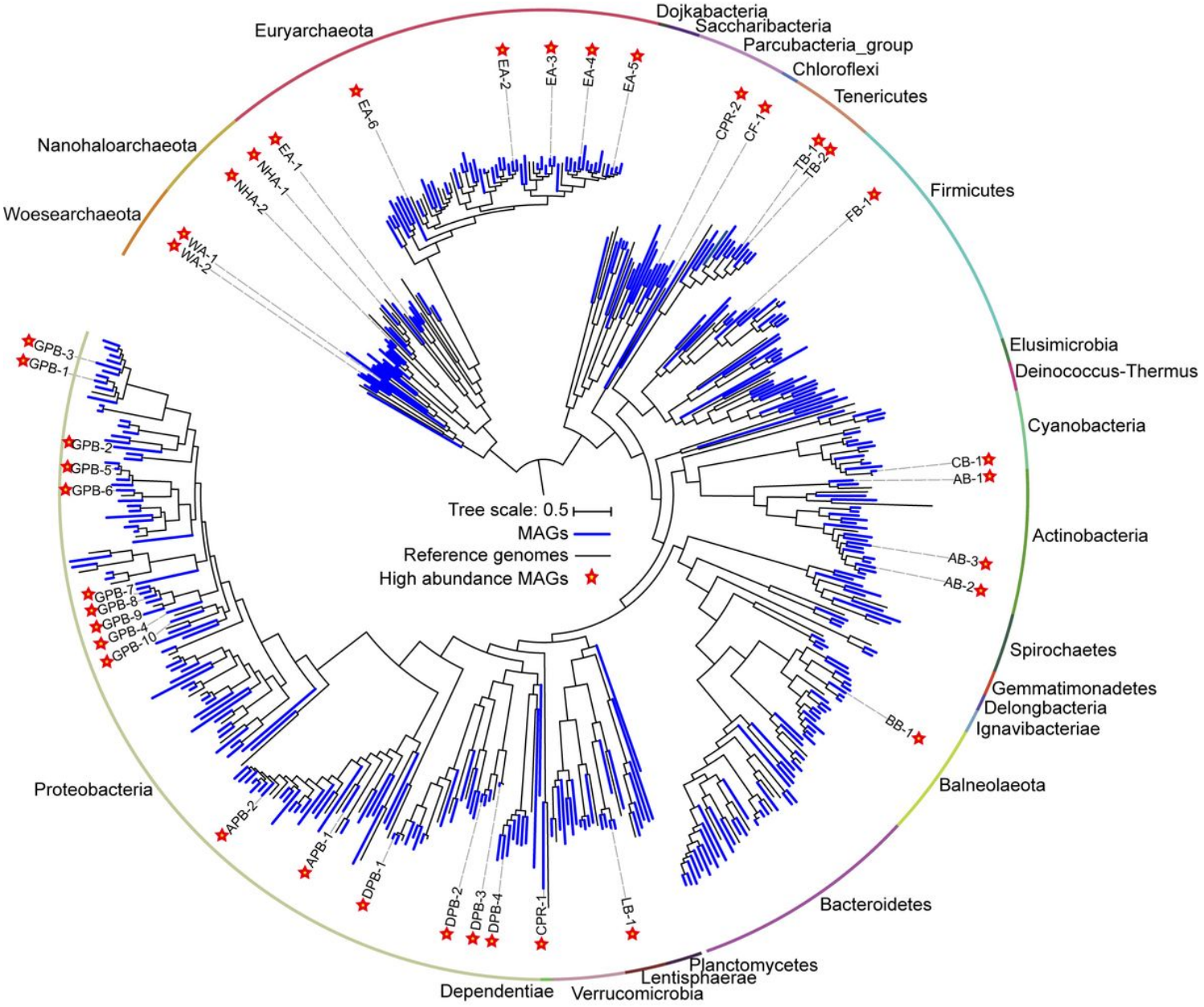

Figure 2

Phylogenomic tree of 385 metagenome-assembled genomes (MAGs) and the evolutionary distribution of abundant MAGs. The MAGs and reference genomes are colored blue and black, respectively. Abundant MAGs are marked with red five-pointed stars. The outer circle is colored by phylum. The complete tree is available with full bootstrap support values in Additional file 4.

Figure 3

The relative abundances of 385 MAGs in 18 samples. The abundance was estimated by the average depth of all contigs in that MAG (Shown in Table S5). The relative abundances of MAGs with the highest

sequence read coverage in each sample were scaled to 100, and MAGs with relative abundances of greater than 50 were considered to be abundant. Blue and red indicate the abundances of MAGs in brine and sediment samples, respectively.

Figure 4

The distribution and metabolic potential of abundant MAGs. Abundant MAGs in brine and sediment samples are colored red and green, respectively. MAGs with metabolic potential are colored in purple. Abbreviation: fxt., fixation; oxd., oxidation; rdc., reduction; disp., disproportionation.

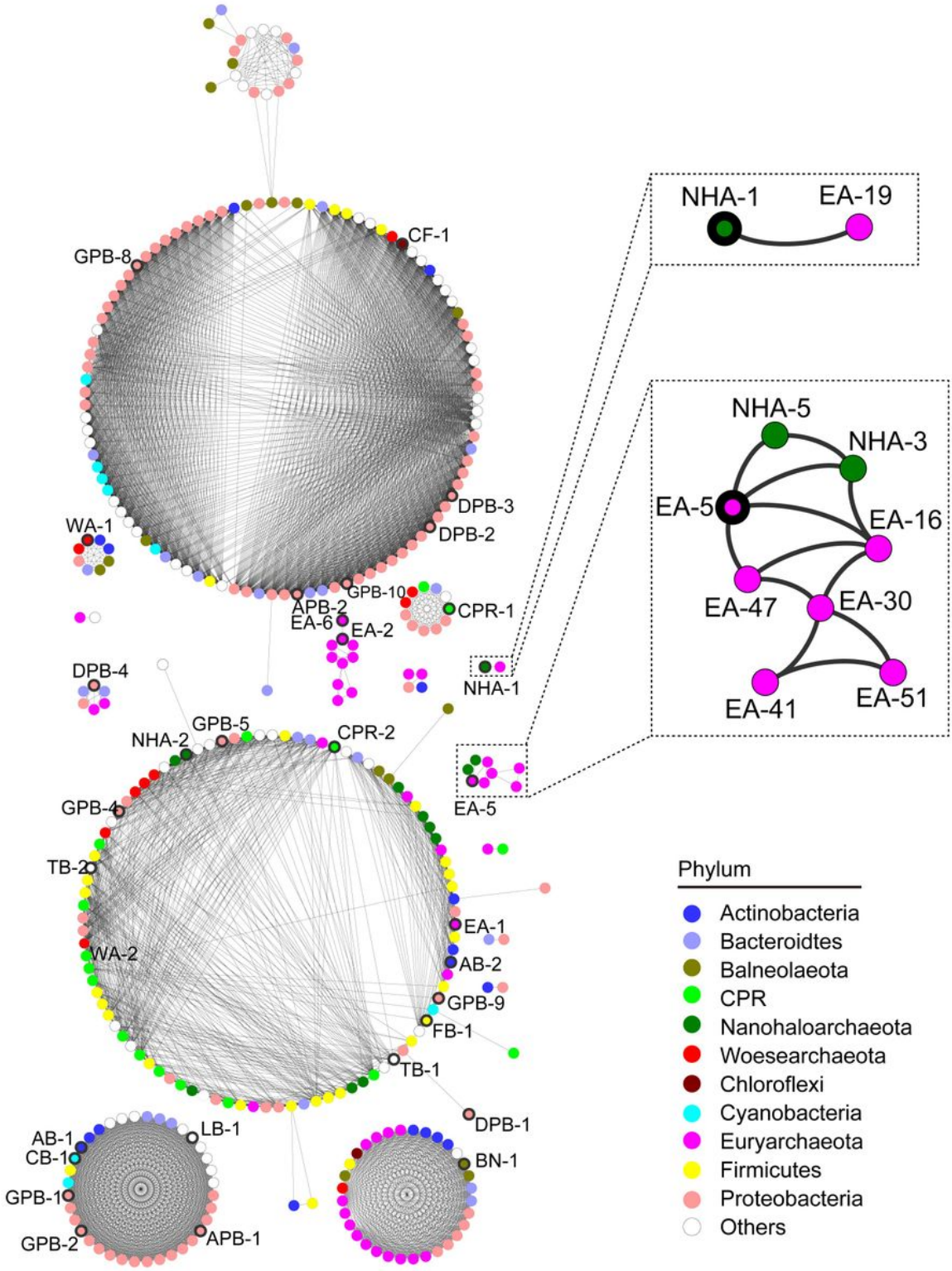

Figure 5

Cooccurrence network based on all 385 MAGs and two Nanohaloarchaeota- containing modules. The coverage of 385 MAGs in 18 samples was used to construct a robust cooccurrence network (Pearson correlation coefficient > 0.9 and p value < 0.01). The nodes in the network are colored by phylum, and the nodes representing abundant MAGs are labeled and bold in the outer ring. Two modules involved are zoomed in to show the robust cooccurrence of Ca. Nanohaloarchaeota and Halobacteria.

Figure 6

Putative fermentation pathways in Candidatus Nanohaloarchaeota and Candidatus Woesearchaeota MAGs. The presence of enzymes was exhibited in detailed (a). We draw the metabolic pathway of carbohydrate fermentation in Candidatus Nanohaloarchaeota (b). Blue and red arrows represented the presence or absence of that pathway in abundant MAG NHA-1. Grey arrow meant the specific transporters were not identified. Biochemical reaction and ATP production of glycolysis via phosphorylation and hydrolysis were compared (c). The metabolic potential of the phosphorylation, hydrolysis and glycolysis pathways are colored purple, yellow and green, respectively. Abbreviation: Amy, alpha-Amylase; Glk, Glucokinase; Pyg, Glycogen phosphorylase (or named 1,4-alpha-glucan phosphorylase); Pgm, phosphoglucomutase; Gpi, Glucose-6-phosphate isomerase; Pfk, 6-Phosphofructokinase; Fba, Fructose-bisphosphate aldolase; Tpi, Triosephosphate isomerase; Gap, Glyceraldehyde 3-phosphate dehydrogenase; Pgk, Phosphoglycerate kinase; Gpm, Phosphoglycerate mutase; Eno, Enolase; Pk, Pyruvate kinase; Glc-1-P, Glucose 1-phosphate; Glc-6-P, Glucose 6-phosphate; Fru-6-P, Fructose 6-phosphate; Fru-1,6-P, Fructose 1,6-biphosphate; Glo-P, Glycerone phosphate; Glh-3-P, Glyceraldehyde 3-phosphate; Gla-3-P, Glycerate 3-phosphate; Gla-2-P, Glycerate 2-phosphate; PEP, Phosphoenolpyruvate; ATP, Adenosine 5'-triphosphate; ADP, Adenosine 5'-diphosphate; NAD+, Nicotinamide adenine dinucleotide; NADH, Reduced nicotinamide adenine dinucleotide; Pi, phosphate.

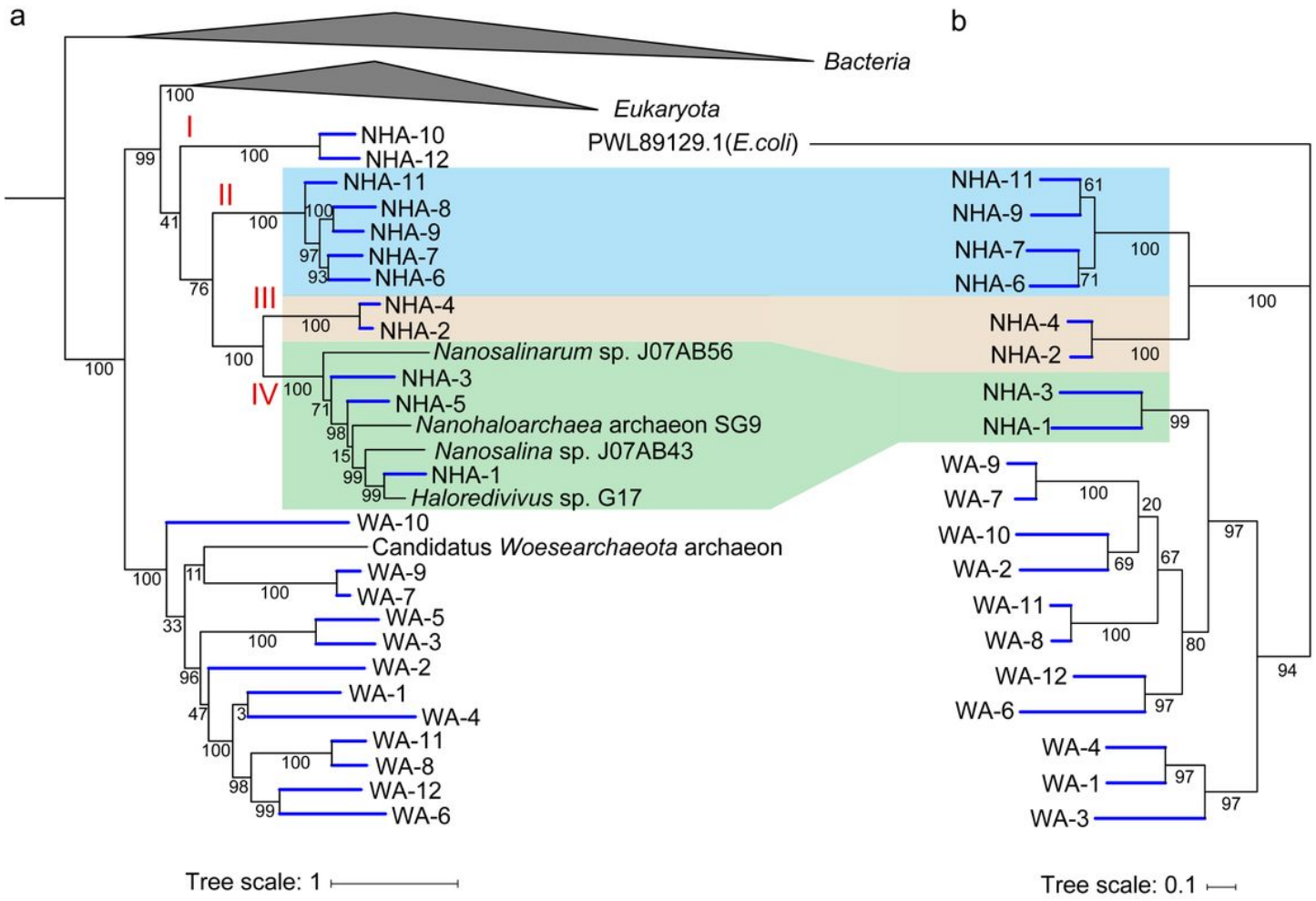

Figure 7

Phylogenetic analysis of amino acid sequences of glycogen phosphorylases obtained from Candidatus Nanohaloarchaeota and Candidatus Woesearchaeota MAGs. a. The tree shown to the left is the phylogenomic tree of 385 MAGs with the reference genome, where the Bacteria and Euryarchaeota branches are collapsed. b. Nineteen predicted glycogen phosphorylases in Nanohaloarchaeota and Woesearchaeota with the alpha-glucan phosphorylase from Escherichia coli (PWL89129.1) were retrieved, aligned and then used to infer the correct tree using the Maximum Likelihood method based on the JTT matrix-based model with MEGA. The tree with the highest log likelihood (-16393.43) is shown with bootstrap support.

Supplementary Files

This is a list of supplementary files associated with this preprint. Click to download.

- Additionalfile4.txt
- Additionalfile5.csv
- Additionalfile3.csv

- Additionalfile1.docx
- Additionalfile2.xlsx